original article

http://www.kidney-international.org

Genetic deletion of the angiotensin-(1–7) receptor Mas leads to glomerular hyperfiltration and microalbuminuria

Sérgio V.B. Pinheiro[1], Anderson J. Ferreira[2], Gregory T. Kitten[2], Kátia D. da Silveira[3], Deivid A. da Silva[1], Sérgio H.S. Santos[3], Elisandra Gava[2], Carlos H. Castro[3], Júnio A. Magalhães[3], Renata K. da Mota[2], Giancarla A. Botelho-Santos[3], Michael Bader[4], Natalia Alenina[4], Robson A.S. Santos[3] and Ana Cristina Simoes e Silva[1]

[1]Pediatric Nephrology Unit, Medicine Faculty, Department of Pediatrics, Federal University of Minas Gerais, Belo Horizonte, Brazil; [2]Department of Morphology, Biological Sciences Institute, Federal University of Minas Gerais, Belo Horizonte, Brazil; [3]Department of Physiology and Biophysics, Biological Sciences Institute, Federal University of Minas Gerais, Belo Horizonte, Brazil and [4]Max Delbrück Center for Molecular Medicine, Berlin, Germany

Angiotensin-(1–7), an active fragment of both angiotensins I and II, generally opposes the vascular and proliferative actions of angiotensin II. Here we evaluated effects of the angiotensin-(1–7) receptor Mas on renal physiology and morphology using Mas-knockout mice. Compared to the wild-type animals, Mas knockout mice had significant reductions in urine volume and fractional sodium excretion without any significant change in free-water clearance. A significantly higher inulin clearance and microalbuminuria concomitant with a reduced renal blood flow suggest that glomerular hyperfiltration occurs in the knockout mice. Histological analysis found reduced glomerular tuft diameter and increased expression of collagen IV and fibronectin in the both the mesangium and interstitium, along with increased collagen III in the interstitium. These fibrogenic changes and the renal dysfunction of the knockout mice were associated with an upregulation of angiotensin II AT1 receptor and transforming growth factor-β mRNA. Our study suggests that Mas acts as a critical regulator of renal fibrogenesis by controlling effects transduced through angiotensin II AT1 receptors in the kidney.

The renin–angiotensin system (RAS) is classically conceived as a coordinated hormonal cascade in the control of cardiovascular, renal, and adrenal functions, mainly through the actions of Angiotensin (Ang)II.[1] Recent advances in cell and molecular biology have led to the recognition of other active fragments of RAS metabolism, such as Ang III, Ang IV, and Ang-(1–7),[2–4] the Ang IV insulin-regulated aminopeptidase-binding site,[5] the angiotensin-converting enzyme (ACE)2, a homolog of classic ACE that forms Ang-(1–7) directly from Ang II and indirectly from Ang I,[6,7] and the G-protein-coupled receptor Mas.[8]

In general, Ang-(1–7) opposes the vascular and proliferative effects of Ang II and exerts complex renal actions in chronic renal diseases and hypertension.[3,9,10] Ang-(1–7) is formed from Ang II by prolylendopeptidase, prolyl-carboxypeptidase or ACE2, or directly from Ang I through hydrolysis by prolylendopeptidase and endopeptidase 24.11 and is metabolized by ACE to Ang-(1–5).[6,7] ACE inhibitors elevate Ang-(1–7) concentrations by both increasing Ang I, a substrate for Ang-(1–7) generation, and preventing Ang-(1–7) degradation.[2–4] Recent studies suggest that, at least in part, the beneficial effects of ACE inhibitors[11,12] and AT1 receptor blockade[13] may be attributed to Ang-(1–7). These findings are in keeping with the hypothesis that the RAS is capable of self-regulating its activity through the formation of Ang-(1–7).[2–4] Furthermore, Kostenis et al[14] showed that receptor Mas can hetero-oligomerize with AT1 and, by so doing, inhibit the actions of Ang II. Indeed, Mas acts in vitro as an antagonist of the AT1 receptor.[15]

Our group showed that deletion of Mas produces an impairment in cardiac function associated with a significant increase in collagen I, III, and fibronectin in the heart.[16] The aim of this study was to evaluate the role of Mas in kidney structure and function using mice with genetic deletion of this receptor.

RESULTS

Renal function parameters

As the results displayed in Table 1 the 24-h urine flow of $Mas^{-/-}$ animals was significantly lower in comparison with that of $Mas^{+/+}$. However, no differences in blood glucose levels and in water and food intake were observed. The reduced urinary volume observed in $Mas^{-/-}$ mice was accompanied by a significant increase in urinary osmolality and a decrease in the fractional excretion of sodium ($P < 0.05$, Table 1). Despite the increase in urinary osmolality, plasma osmolality, osmolal, and free-water clearance were unchanged in $Mas^{-/-}$ animals when compared with those in $Mas^{+/+}$ mice. No changes were detected in the fractional excretion of potassium either. Mean arterial pressure (MAP) in $Mas^{-/-}$ mice was also undistinguished from that in $Mas^{+/+}$ animals. However, significant reductions of renal blood flow accompanied by increased total renal vascular resistance were detected in knockout mice. Despite the reduced renal blood flow, $Mas^{-/-}$ animals presented a significant elevation in the glomerular filtration rate (GFR), estimated by the creatinine and inulin clearances. This finding was made along with an elevated urinary albumin excretion in $Mas^{-/-}$ mice ($P < 0.05$, Table 1).

Renal structure

The wet weights of kidneys from $Mas^{+/+}$ and $Mas^{-/-}$ animals normalized for body weight (BW) were similar (Table 2). However, microscopic changes in the kidney structure of $Mas^{-/-}$ mice were observed, including a significant reduction in the diameters of the glomerular tuft and Bowman's capsule in comparison with those in $Mas^{+/+}$ animals (Figure 1 and Table 2). Bowman's spaces and the diameter of the cortical tubule were unaltered in $Mas^{-/-}$ animals when compared with those in $Mas^{+/+}$ mice.

Renal tissue analysis by confocal microscopy revealed that the fluorescence of many extracellular matrix proteins was significantly higher in the cortex and medulla of $Mas^{-/-}$ kidneys when compared with those in $Mas^{+/+}$ (Figures 2 and 3). $Mas^{-/-}$ kidneys exhibited a significant increase in collagen III in the cortex (9.08 ± 1.63 versus 1.83 ± 0.77 arbitrary units in $Mas^{+/+}$ mice, $P < 0.05$, Figure 2) as well as in the medulla (3.60 ± 0.79 versus 0.26 ± 0.05 arbitrary units in $Mas^{+/+}$ mice, $P < 0.05$, Figure 3). Similar results were obtained with collagen IV and fibronectin. Kidneys from $Mas^{-/-}$ animals presented higher levels of both extracellular matrix proteins than did $Mas^{+/+}$ kidneys in the renal cortex (collagen IV: 8.49 ± 0.61 versus 6.49 ± 0.43 arbitrary units and fibronectin: 11.22 ± 2.40 versus 4.07 ± 0.47 arbitrary units, $P < 0.05$ for both comparisons, Figure 2) and medulla (collagen IV: 18.98 ± 1.11 versus 10.70 ± 0.84 arbitrary units and fibronectin: 21.56 ± 2.71 versus 11.04 ± 2.24 arbitrary

Table 2 | Morphological parameters in Mas$^{+/+}$ and Mas$^{-/-}$ mice

Parameters	Mas$^{+/+}$	Mas$^{-/-}$
Kidney index (mg/g of body weight)	6.0 (5.6–6.4)	5.9 (5.5–6.3)
Cortical tubule diameter (μm)	32.5 (30.0–37.5)	32.5 (30–37.5)
Bowman's capsule diameter (μm)	62.5 (57.5–70.0)	57.5 (52.5–62.5)*
Glomerulus tuft diameter (μm)	57.5 (52.5–62.5)	50.0 (47.5–55.0)*
Bowman's space diameter (μm)	6.0 (5.7–6.3)	6.1 (5.8–6.3)

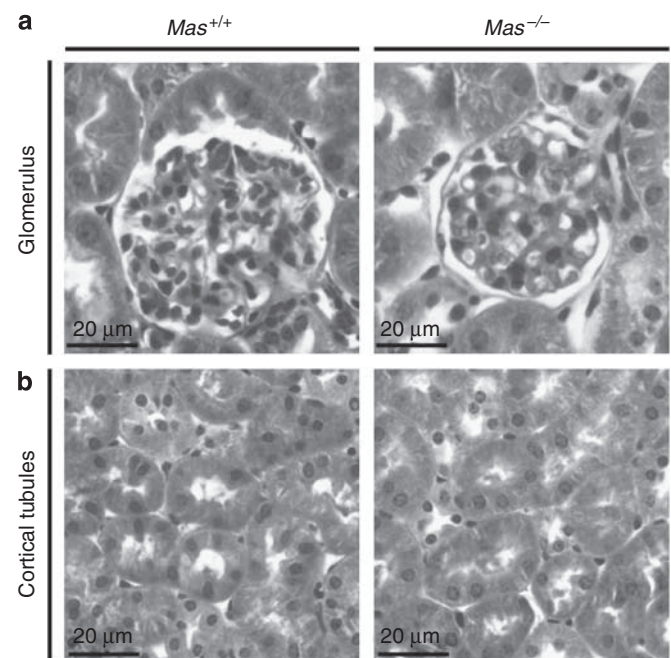Values are medians (25 and 75% percentile), *$P < 0.05$. Data were analyzed by the Mann–Whitney test.

Table 1 | General measurements and renal function parameters in Mas$^{+/+}$ and Mas$^{-/-}$ mice

Parameters	Mas$^{+/+}$	Mas$^{-/-}$
Body weight (g)	25.7 ± 0.5	25.7 ± 0.6
Blood glucose (mg per 100 ml)	116.8 ± 3.9	111.8 ± 3.2
Daily food intake (g)	5.18 ± 0.25	5.69 ± 0.27
Daily water intake (ml)	6.37 ± 0.34	5.90 ± 0.32
Daily urine volume (ml)	1.65 ± 0.19	1.07 ± 0.14*
Mean arterial pressure (mm Hg)	80.22 ± 1.78	78.75 ± 2.23
RBF (ml/min per g)	19.16 ± 4.09	10.76 ± 1.39*
RVR (mm Hg ml/min per g)	5.39 ± 1.20	8.25 ± 1.07*
Creatinine clearance (μl/min per g)	1.80 ± 0.39	3.20 ± 0.50*
Inulin clearance (μl/min per g)	2.54 ± 0.49	4.61 ± 0.74*
Microalbuminuria (mg per 24 h)	0.03 ± 0.01	0.20 ± 0.07*
Urine osmolality (mOsm/kg H$_2$O)	3245 ± 196	4030 ± 330*
Serum osmolality (mOsm/kg H$_2$O)	275 ± 7	273 ± 5
Osmolal clearance (μl/min)	10.2 ± 0.8	9.1 ± 0.8
Free water clearance (μl/min)	-9.2 ± 0.7	-8.4 ± 0.7
Serum sodium (mmol/l)	149 ± 2	147 ± 2
Sodium FE (%)	1.05 ± 0.14	0.38 ± 0.05*
Serum potassium (mmol/l)	4.8 ± 0.4	5.1 ± 0.4
Potassium FE (%)	15.5 ± 3.5	15.3 ± 5.6

FE, fractional excretion; RBF, renal blood flow; RVR, renal vascular resistance. Values are mean $\pm$ s.e.m. *$P < 0.05$. Data were analyzed by unpaired Student's t-test.

Figure 1 | Kidney architecture in Mas$^{+/+}$ and Mas$^{-/-}$ mice. Kidney sections showing reduced Bowman's capsule and glomeruli tuft in $Mas^{-/-}$ mice in comparison with $Mas^{+/+}$ controls (Masson's trichrome, $\times 400$).

units, $P < 0.05$ for both comparisons, Figure 3). However, no differences in the expression of collagen I in the cortex and medulla were observed in the kidneys from $Mas^{-/-}$ and

a

$Mas^{+/+}$ $Mas^{-/-}$

Col I

Col III

Col IV

Fn

b

Analysis
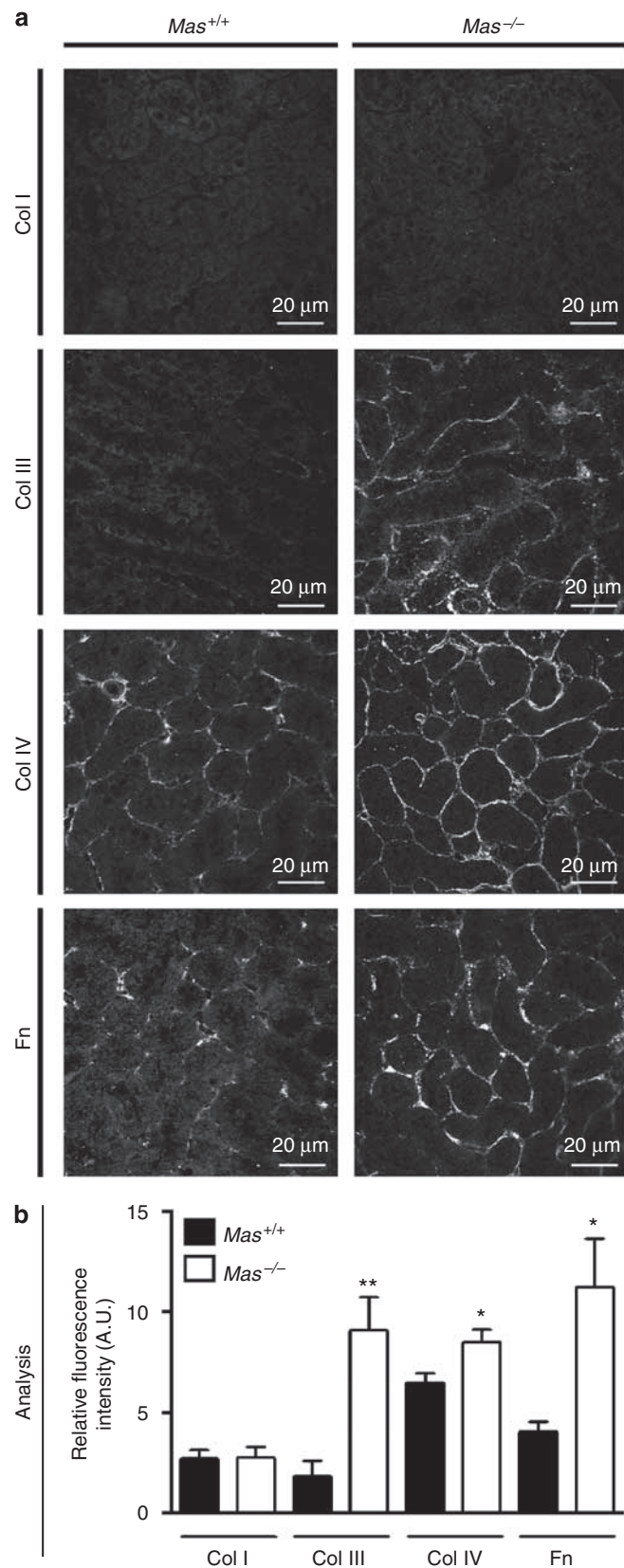
$Mas^{+/+}$ animals (Figures 2 and 3). In the mesangium, $Mas^{-/-}$ kidneys exhibited a selective increase in collagen IV (13.25 ± 0.99 versus 10.07 ± 0.60 arbitrary units in $Mas^{+/+}$ mice, $P < 0.05$) and fibronectin (29.43 ± 4.17 versus 14.22 ± 2.66 arbitrary units in $Mas^{+/+}$ mice, $P < 0.05$). In contrast, collagen types I and III exhibited a similar pattern in the mesangium in $Mas^{-/-}$ and $Mas^{+/+}$ kidneys (Figure 4). As shown in Figure 5, results obtained with immunoblotting confirmed the increased levels of fibronectin and collagen types III and IV in $Mas^{-/-}$ animals.

Distribution of Mas in the kidney
To determine the distribution of Mas in the kidneys, confocal immunofluorescence analysis of renal tissue from $Mas^{+/+}$ mice was performed. Mas immunolabeling was detected in different segments of the nephron, such as the juxtaglomerular apparatus, proximal cortical tubules, and collecting ducts (Figure 6).

AT$_1$ receptor and TGF-β RNA expression in the kidney
As observed in Figure 7, real-time PCR revealed a threefold increase in RNA expression of AT$_1$ receptor and a twofold elevation of total transforming growth factor-β (TGF-β) RNA in kidneys from $Mas^{-/-}$ mice compared with those in $Mas^{+/+}$ mice (2.65 ± 0.29 versus 0.85 ± 0.19 relative expression for AT$_1$ RNA and 1.75 ± 0.23 versus 0.85 ± 0.17 relative expression for TGF-β RNA, $P < 0.05$ for both comparisons).

DISCUSSION
Genetic deletion of the Ang-(1–7) receptor Mas produces an extremely rich phenotype that includes cardiac dysfunction,[16] decreased baroreflex function, endothelial dysfunction,[17] reduced reproductive function,[18] increased thrombogenesis,[19] and, depending on the genetic background, increased blood pressure and marked changes in lipid and glycidic metabolism, leading to a metabolic syndrome-like state.[17,20]

Phenotypic differences have been reported according to genetic background. This is particularly true for blood pressure and plasma glucose, which are increased in FVB/N $Mas^{-/-}$[17,20] and are normal in C57BL/6 mice, as shown in this study. These differences could be related to the fact that C57BL/6 presents only one renin gene compared with two genes of other mice strains, including FVB/N.[21] However, despite the potentially lower sensitivity to the genetic deletion of Mas in C57BL/6 mice, we showed that Mas is critical for

Figure 2 | Immunofluorescence of extracellular matrix (ECM) proteins in the cortex of kidneys from $Mas^{+/+}$ (left column) and $Mas^{-/-}$ (right column) mice. (**a**) Fluorescence (Cy3-labeled anti-rabbit IgG) reveals the immunolabeling of ECM proteins. Expression of type III collagen (Col III), type IV collagen (Col IV), and fibronectin (Fn) were increased in the cortex of $Mas^{-/-}$ compared with that of $Mas^{+/+}$ mice, whereas the expression of type I collagen (Col I) was unaltered. (**b**) Quantification of ECM proteins in the cortex of $Mas^{+/+}$ and $Mas^{-/-}$ mice. Data are shown as mean ± s.e.m. *$P < 0.05$; **$P < 0.01$. A.U. indicates arbitrary unit.

the regulation of renal homeostasis even in young animals. Our data suggest that the genetic deletion of *Mas* probably leads to glomerular hypertension, and also produces structural and molecular changes, which stimulates renal

Figure 3 | Immunofluorescence of extracellular matrix (ECM) proteins in the medulla of kidneys from *Mas*^{+/+} (left column) and *Mas*^{−/−} (right column) mice. (**a**) Fluorescence (Cy3-labeled anti-rabbit IgG) reveals the immunolabeling of ECM proteins. Expression of type III collagen (Col III), type IV collagen (Col IV), and fibronectin (Fn) were increased in the medulla of *Mas*^{−/−} compared with that of *Mas*^{+/+} mice, whereas the expression of type I collagen (Col I) was unaltered. (**b**) Quantification of ECM proteins in the medulla of *Mas*^{+/+} and *Mas*^{−/−} mice. Data are shown as mean ± s.e.m. *$P < 0.05$; **$P < 0.01$. A.U. indicates arbitrary unit.

fibrosis. Furthermore, the observed changes were not related to arterial hypertension or to hyperglycemia.

The ability of the kidney to generate high concentrations of Ang II and Ang-(1–7) allows it to regulate intrarenal levels of these angiotensins in accordance with homeostatic needs for the regulation of renal hemodynamics.[22,23] In this context, *Mas*-deficient mice presented significant changes in renal hemodynamic and in glomerular filtration. When compared with wild-type mice, *Mas*^{−/−} animals had lower renal blood flow accompanied by elevated renal vascular resistance. Both alterations occurred along with a 1.8-fold increase in GFR according to creatinine as well as inulin clearance measurements, and a 6.7-fold increase in urinary albumin excretion. As blood pressure was similar in *Mas*^{−/−} and in wild-type animals, the increased GFR in conjunction with reduced renal blood flow was probably because of elevated vascular tonus in the efferent arterioles. Ang II markedly raises efferent glomerular arteriolar resistance but does not change afferent arteriolar resistance unless the renal perfusion pressure rises.[24] The consequence of the disproportionate increase in efferent (over afferent) resistance is a marked increase in intraglomerular pressure. Thus, the Ang II-induced decrease in renal plasma flow is offset by the increase in mean transcapillary ultrafiltration pressure and this maintains or even increases the GFR.[22–25] Ang-(1–7) directly and indirectly vasodilates afferent arterioles and increases renal blood flow.[26–28] Although the relative role of each angiotensin on glomerular hemodynamics is still unknown, our results indicated that Ang-(1–7) may act as a physiological regulator of intraglomerular pressure by opposing the glomerular hypertensive effects of Ang II. Therefore, without the physiological antagonism of Ang-(1–7), intrarenal and/or plasma Ang II, acting on higher expressed AT_1 receptors, might increase efferent arteriolar resistance and glomerular filtration pressure, thus contributing to glomerular capillary hypertension.

Mas-knockout animals also exhibited lower urinary volume accompanied by sodium retention without BW gain when compared with controls. As young *Mas*^{−/−} mice (9–10 weeks of age) were used, it would be possible that the persistence of these alterations could lead to edema and BW elevations in older animals. Moreover, no changes in serum osmolality, osmolal, or free-water clearance were observed, indicating that fluid retention reflects a direct effect on
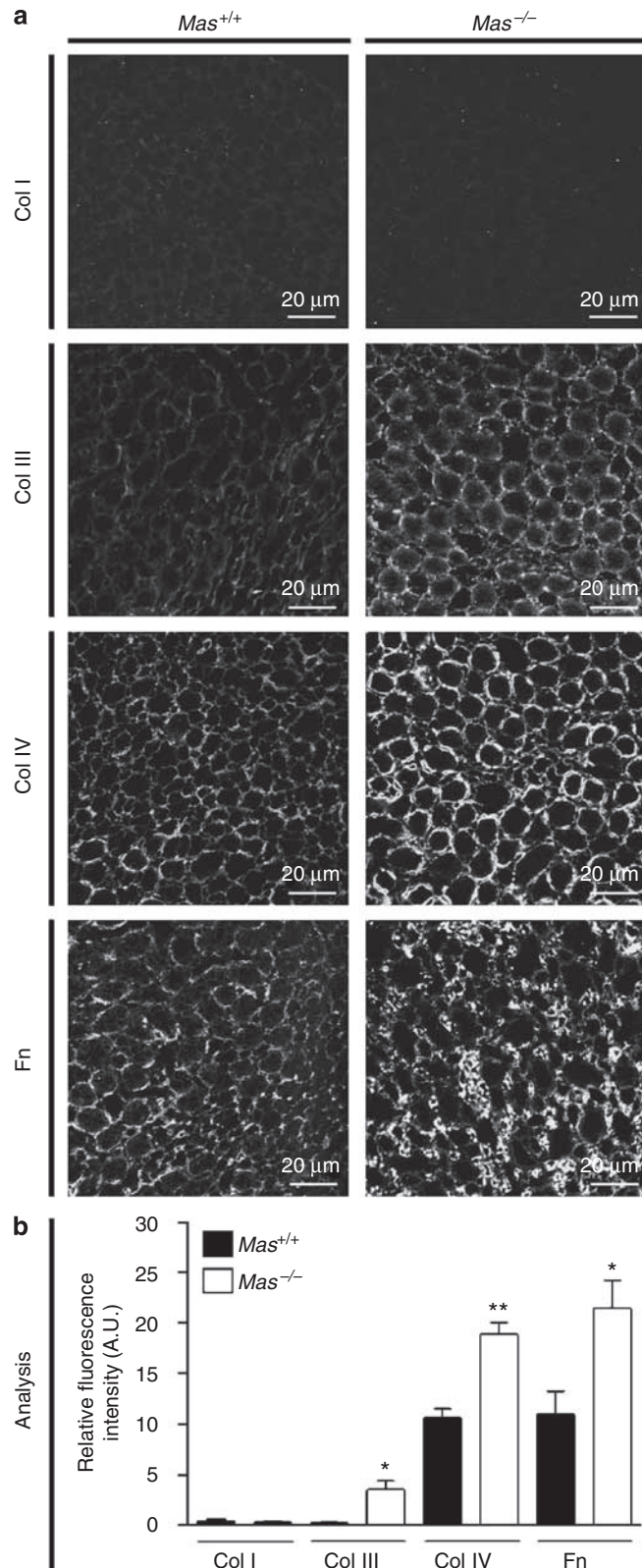
sodium handling without significant changes in water transport.[29] These alterations are in agreement with the tubular effects of Ang II.[25] Through efferent arteriolar

a

b

vasoconstriction, Ang II causes changes in peritubular capillary dynamics that could increase renal tubular fluid reabsorption.[24,25] In addition, Ang II significantly stimulates proximal and distal sodium reabsorption through the activation of AT_1 receptors.[22,23] Although further experiments with AT_1 blockade would be helpful, our findings suggest that ACE–Ang II–AT_1 axis could influence the direction of renal tubular changes detected in $Mas^{-/-}$ mice.

The major morphological alterations found in kidneys from young $Mas^{-/-}$ animals were a reduction in glomerular tuft diameter and an increased expression of collagen III, IV, and fibronectin in the kidney interstitium as well as of collagen IV and fibronectin in the mesangium. Despite the presence of matrix proteins deposition in kidneys of $Mas^{-/-}$ mice, we did not observe the classical findings of glomerular hypertension, such as glomerular hyperthrophy. However, as this study reflected only a time point after *Mas* deletion (9- to 10-week-old mice), we were not able to show dynamic changes in glomerular size. Glomerular hypertrophy may not be evident in young animals. Similarly, the kidneys of young (3-month-old) mice with the deletion of *ACE2* gene showed no gross abnormalities having normal architecture of the cortex and medulla, comparable with those of age-matched wild-type mice. However, electron microscopy of these mice evidenced mesangial injury with small foci of collagen deposition suggestive of an early disease process.[30] We also cannot rule out the possibility that the genetic deletion of Mas could interfere with fetal glomerular development by producing smaller glomerulus than that of wild-type animals. Consequently, even if glomerular hypertrophy has occurred in $Mas^{-/-}$ mice, it might not be detected. Further studies are obviously necessary to clarify the time course of histological glomerular changes in $Mas^{-/-}$ animals. In addition, changes in glomerular permeability, not evaluated in this study, may be also involved in the glomerular dysfunction present in $Mas^{-/-}$ mice.

Our earlier studies have indicated a role for the Ang-(1–7)–Mas interaction in the regulation of matrix proteins deposition in the heart and liver.[16,31] In this study, we showed the fibronectin and collagen III deposition in the kidney of young $Mas^{-/-}$ mice, suggesting an initial fibrogenic process. Accordingly, in the initial stages of collagen deposition and renal fibrosis, type III collagen appears in greater amounts than do type I.[32,33] As fibrogenesis progresses, there is a
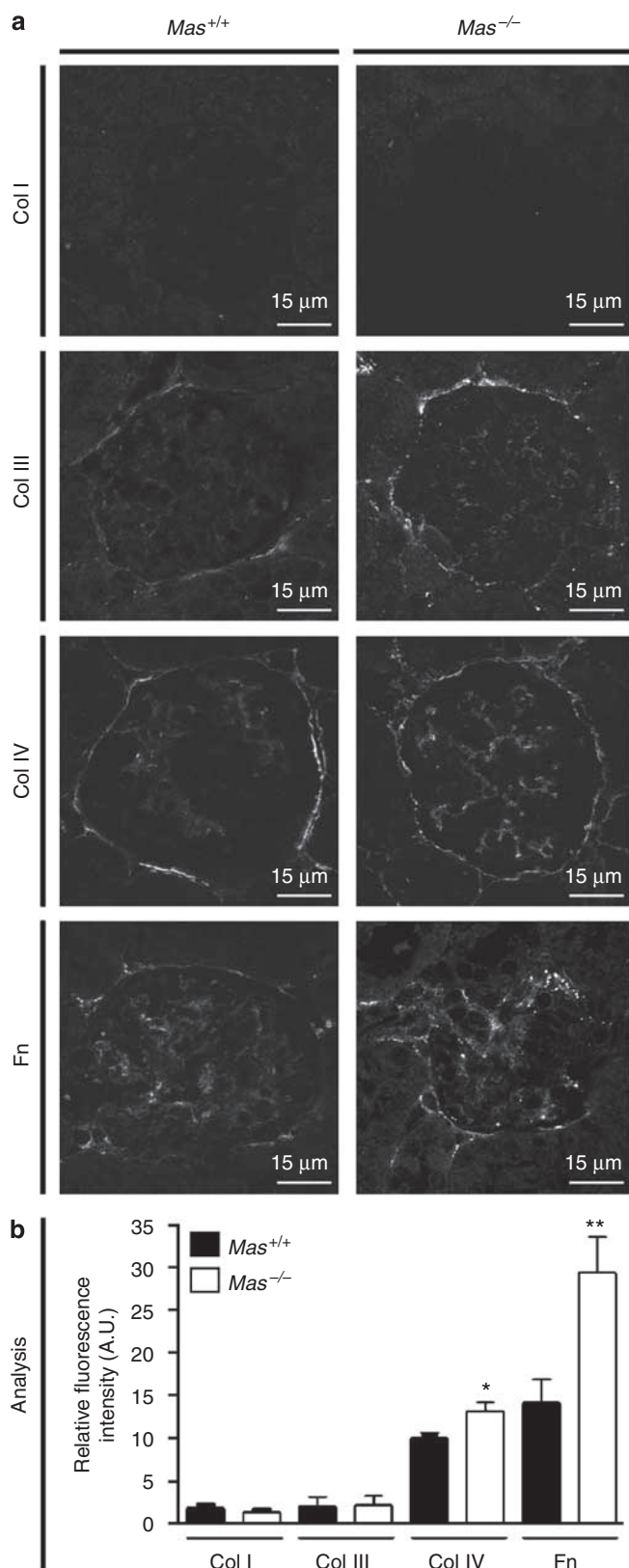
Figure 4 | Immunofluorescence of extracellular matrix (ECM) proteins in the mesangium of kidneys from $Mas^{+/+}$ (left column) and $Mas^{-/-}$ (right column) mice. (**a**) Fluorescence (Cy3-labeled anti-rabbit IgG) reveals the immunolabeling of ECM proteins. Expression of type IV collagen (Col IV) and fibronectin (Fn) was increased in the mesangium of $Mas^{-/-}$ compared with $Mas^{+/+}$ mice, whereas the expression of type I collagen (Col I) and type III collagen (Col III) was unaltered. (**b**) Quantification of ECM proteins in the mesangium of $Mas^{+/+}$ and $Mas^{-/-}$ mice. Data are shown as the mean ± s.e.m. *$P < 0.05$; **$P < 0.01$. A.U. indicates arbitrary unit.
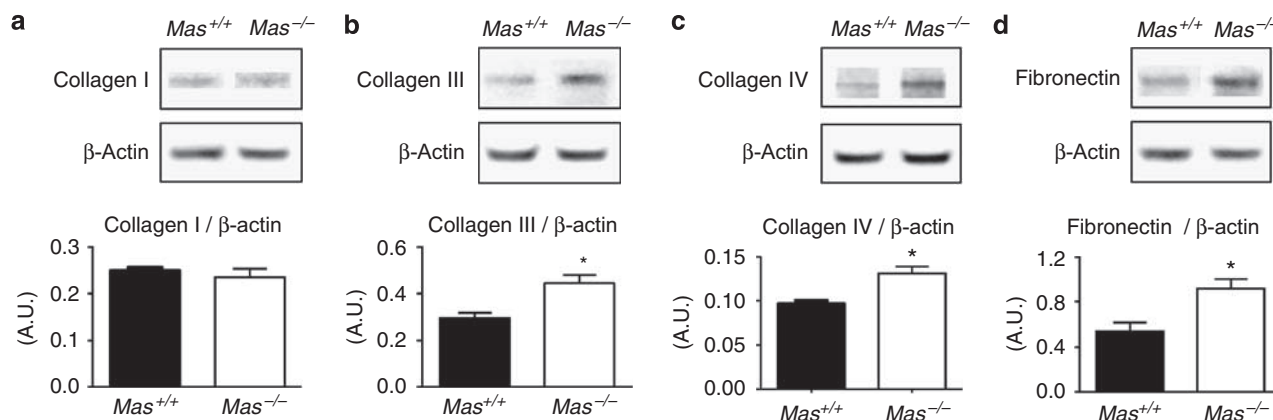
Figure 5 | Immunoblotting of extracellular matrix (ECM) proteins in kidneys of Mas$^{+/+}$ and Mas$^{-/-}$ animals. (a) Immunoblotting shows no difference of Collagen I expression in Mas$^{+/+}$ and Mas$^{-/-}$ mice kidneys. Significant increases in (b) Collagen III, (c) Collagen IV, and (d) fibronectin expression were detected by comparing immunoblots of Mas$^{-/-}$ mouse kidneys with those of Mas$^{+/+}$ controls. Each band represents one mouse kidney from either Mas$^{+/+}$ or Mas$^{-/-}$ mice. Data are shown as the mean ± s.e.m. *$P < 0.05$. A.U. indicates arbitrary unit.
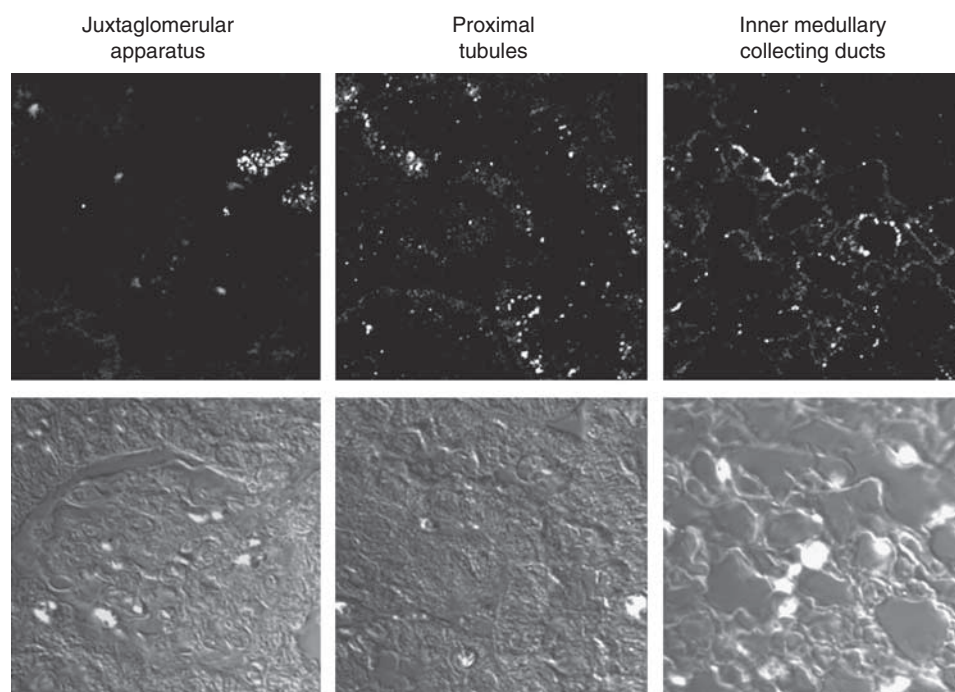

Figure 6 | Immunofluorescence of Mas receptor in the kidney of Mas$^{+/+}$ control mice. Fluorescence (Cy3-labeled anti-rabbit IgG) reveals the immunolabeling of Mas antibody in kidney tissue.

proportional decrease in type III collagen, and tubulointerstitial fibroblasts secrete collagen types I, III, IV, and V in response to TGF-β, epidermal growth factor, and interleukin-2.[32,33] Several studies have shown the involvement of the Ang II–AT$_1$ axis in profibrotic mechanisms.[34–38] Ang II is the key mediator of many processes involved in glomerulosclerosis, affecting blood pressure, glomerular hemodynamics, and matrix proteins deposition.[38] Moreover, the improvement in renal function and the regression of renal fibrosis during RAS antagonism largely involve a decreased collagen expression mediated by the Ang II–TGF-β pathway, but other mechanisms may also play a role.[38–42]

Although a protective role for Ang-(1–7) in renal fibrosis remains speculative, we provide strong evidence for such a role by showing alterations in renal structure because of the absence of Mas. In this regard, many studies have shown that Ang-(1–7) exerts inhibitory effects on vascular and cellular growth mechanisms.[31,43–46] The molecular mechanisms for the antiproliferative response to Ang-(1–7) include the stimulation of prostaglandin and cAMP production as well as the inhibition of mitogen-activated protein (MAP) kinases.[45] Mas seems to mediate the antiproliferative effect of Ang-(1–7) in vascular smooth muscle cells,[43] liver tissue,[31] and cardiomyocytes.[47] Moreover, Mas-deficient mice
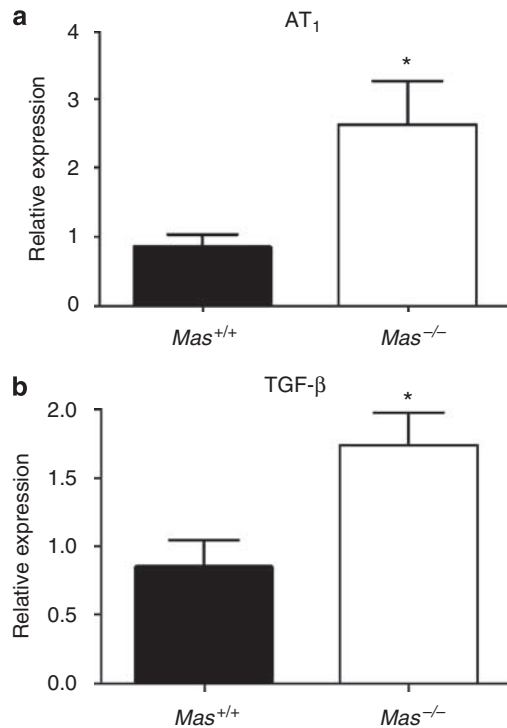
a

b

Figure 7 | Total RNA expression of AT$_1$ receptor and transforming growth factor-β (TGF-β) in mouse kidneys. (a) Relative expression of AT$_1$ receptor RNA in the kidneys of $Mas^{+/+}$ and $Mas^{-/-}$ mice. **(b)** Relative expression of TGF-β RNA in the kidneys of $Mas^{+/+}$ and $Mas^{-/-}$ mice. Data are shown as mean ± s.e.m. *$P < 0.05$.

exhibited an impairment of heart function associated with changes in collagen expression toward a profibrotic profile.[16] Gallagher and Tallant[46] also reported the inhibition of human lung cell growth by Ang-(1–7) through a reduction in the serum-stimulated phosphorylation of extracellular signal-regulated kinase (ERK) 1 and ERK2. As the ERK cascade is activated in response to different stimuli, such as growth factors, cytokines, or DNA-damaging agents, the stimulation of the ACE2–Ang-(1–7)–Mas axis could be effective in halting glomerulosclerosis. Su *et al*[48] have reported that Ang-(1–7) inhibits Ang II-stimulated MAP kinases phosphorylation in proximal tubular cells. Thus, the generation of Ang-(1–7) by proximal tubular ACE2 could counteract the proliferative effects of locally produced Ang II.[48] In keeping with this possibility, recent studies suggested a protective role for ACE2 in the kidney.[30,49–52] Kidney diseases have been associated with a reduction in renal ACE2 expression, possibly facilitating the damaging effects of Ang II.[30,49–52] Acquired or genetic ACE2 deficiency also appears to exacerbate renal damage and albuminuria in experimental models, supporting this hypothesis.[30,50–52] In addition, chronic blockade of ACE2 with the enzyme inhibitor, MLN-4760, in control or diabetic mice produced albuminuria and matrix proteins deposition.[52] Taken together, these findings suggest that a decrease in ACE2 may be involved in kidney disease, possibly by disrupting the metabolism of angiotensin peptides. It is not clear yet,

however, whether this effect is because of degradation of Ang II, formation of Ang-(1–7), or presumably both.

Angiotensin II clearly exerts a key role in the progression of renal diseases, justifying the use of RAS inhibition to reduce the rate of renal function loss and to ameliorate renal fibrosis.[53,54] Clinical studies have shown that ACE inhibitors and AT$_1$ receptor antagonists delay the progression of chronic kidney disease to end-stage renal disease.[1,53–56] It should be mentioned that Ang-(1–7) levels have significantly increased during chronic treatment with ACEIs or AT$_1$ blockers.[10,13] However, the cellular and molecular mechanisms involved in RAS inhibition are not fully understood. In this regard, we also found an increased expression of AT$_1$ receptor and TGF-β RNA in *Mas* knockout animals as compared with those in controls. These results indicate a molecular deviation toward a fibrogenic process because of the blunted activity of the ACE2–Ang-(1–7)–Mas axis and an unopposed action of the Ang II–AT$_1$ axis at the renal level. Corroborating our hypothesis, Kostenis *et al*[14] suggest that Mas is a physiological antagonist of the AT$_1$ receptor. These authors also described that Mas and AT$_1$ can form a constitutive hetero-oligomeric complex that is unaffected by the presence of agonists or antagonists of both receptors.[14] Moreover, mice lacking the *Mas* gene showed enhanced Ang II-mediated vasoconstriction in mesenteric microvessels *in vivo*.[14]

In summary, our findings suggest that the lack of Mas produced a RAS imbalance leading to abnormal predominance of the ACE–Ang II–AT$_1$ axis. Consequently, $Mas^{-/-}$ mice presented sodium and water retention, renal fibrosis and inflammation, glomerular hyperfiltration, proteinuria, and a tendency toward glomerulosclerosis. The ACE2–Ang-(1–7)–Mas axis should be further investigated for the treatment of renal fibrosis.

MATERIALS AND METHODS
Animals
Nine- to 10-week-old male C57BL/6 wild-type ($Mas^{+/+}$) and C57BL/6 *Mas*-knockout mice ($Mas^{-/-}$) were obtained from the transgenic animal facilities of our Institution. The study was approved by our Ethics Committee.

General measurements and renal function parameters
To evaluate the effects of Mas deletion on renal physiology, $Mas^{+/+}$ ($n = 18$) and $Mas^{-/-}$ ($n = 17$) mice were compared. The animals were kept in a temperature-controlled room on a 14/10h-light/dark cycle and housed in individual metabolic cages, with free access to standard chow and tap water. After an adaptation period of 48 h, urine volume, water, and food intake were measured for the next 24 h. At the end, 24h-urine samples were collected and centrifuged at 3000 g for 5 min. Urine was used to determine osmolality, microalbuminuria, sodium, potassium, and creatinine concentrations. Blood samples were also obtained by decapitation and centrifuged at 2000 g for 10 min. The resulting plasma was used to measure osmolality, glucose, sodium, potassium, and creatinine concentrations.

Sodium and potassium levels were measured by flame-photometry (Barueri, SP, Brazil) (Celm FC-180, USA); creatinine concentration was determined by an enzymatic kit (Labtest,

Belo Horizonte, MG, Brazil); glucose levels were measured by Accu-Check glucometer (Roche Diagnostics, Indianapolis, IN, USA); microalbuminuria was determined by a latex immunoassay (Gold Analisa, Belo Horizonte, MG, Brazil); and osmolality was determined by a freezing-point osmometer (microOsmette, Calumet City, IL, USA). Urinary fractional excretion of sodium and potassium, osmolal clearance, free-water clearance, and creatinine clearance were calculated.

To confirm the GFR estimated by creatinine clearance, plasma inulin elimination kinetic was determined following a single bolus injection of inulin[57] in an additional group of $Mas^{+/+}$ ($n = 7$) and $Mas^{-/-}$ ($n = 7$) mice. The plasma inulin concentration was measured at 5, 10, 20, and 45 min after bolus injection by the antron method.[58] Inulin clearance was analyzed by using one-compartment model according to the formula: Inulin clearance $= I/(A/\alpha)$, where I is inulin quantity, A is the y-intercept value of the decay rate and α is the decay constant. A nonlinear regression curve-fitting program (GraphPad Prism Software, USA) performed all calculations.

Mean arterial pressure, renal blood flow, and total renal vascular resistance were determined in an additional group of $Mas^{+/+}$ ($n = 10$) and $Mas^{-/-}$ ($n = 10$) mice. MAP was recorded through a femoral arterial catheter connected to a data acquisition system (MP100-BIOPAC System Inc., Goleta, CA, USA). After 15 min of baseline MAP record, renal blood flow was measured by the fluorescent polystyrene microspheres (Molecular Probes, Invitrogen Corporation, Carlsbad, CA, USA) technique.[59–61] Briefly, two different colors of 15 μm fluorescent microspheres were selected to avoid spillover between colors.[59] After mixing, 50,000 (50 μl) fluorescent microspheres were infused into the left ventricle over 10 s. To calculate blood flow, arterial blood was withdrawn at a rate of 0.25 ml/min through the right femoral artery for 55 s, starting 10 s before microspheres injection. In the end, the animals were killed by lethal anesthesia. Kidneys were then removed, weighed, and placed in individual vials. Tissue and reference blood flow samples were digested by 4 M ethanol-KOH and 2% Tween 80 solution and kept in a hot bath (50°C) overnight. The microspheres were then recovered by the sedimentation method[60] and the dye was extracted with 4 ml of an organic solvent ethyl-acetate. The fluorescence intensity was measured by luminescence spectrophotometry (Spex Fluoromax, HORIBA Jobin Yvon Inc., Edison, NJ, USA) and renal blood flow was calculated, as described earlier.[59–61] The total renal vascular resistance was calculated by the ratio between MAP and renal blood flow of each animal.

Renal structure

To evaluate renal structure, histomorphometrical, immunohistochemical, and immunoblotting analyses were performed on kidneys from $Mas^{+/+}$ ($n = 4$) and $Mas^{-/-}$ ($n = 4$) mice.

Histomorphometry. Both kidneys of each animal were immediately removed; mean wet weights were recorded and normalized for BW (mg/g). Kidneys from each group were left in 4% Bouin fixative for 24 h at room temperature. The tissues were dehydrated by sequential washes with graded ethanol concentrations and embedded in paraffin. Cross–sections (5 μm) were cut from the middle area of the kidney and stained with Masson's trichrome. The tissue sections were examined under light microscope (BX60, Olympus, Center Valley, PA, USA) at × 400 magnification and photographed (Qcolor3, Olympus). The diameter of Bowman's capsule and the glomerular tuft from the glomerulus cut in vascular pole planes (mean of 15 glomeruli per kidney) as well as the

diameter of the proximal cortical tubules (mean of 40 segments per kidney) were analyzed using Image Pro-Express software.

Immunohistochemistry. Immunofluorescence-labeling and quantitative confocal microscopy evaluated the distribution and amount of collagen types I, III, IV, and fibronectin in $Mas^{+/+}$ and $Mas^{-/-}$ mice kidneys. The same methodology was described earlier for collagen I and III in human scars and normal skins.[62] Briefly, the kidneys were obtained from $Mas^{+/+}$ and $Mas^{-/-}$ mice, washed in phosphate-buffered saline to eliminate blood, and cryofixed in 80% methanol and 20% dimethyl-sulfoxide at −80°C. The samples were stored at −80°C for 7 days, moved to −20°C for 1 day, washed thrice in 99.9% ethanol at room temperature, twice in xylene, and then embedded in paraffin. Sections of 5–8 μm were mounted on slides, deparaffinized with xylene, rehydrated through graded series of ethanol to phosphate-buffered saline and then incubated in a blocking solution (1% bovine serum albumin and 0.1% Tween 20) at room temperature for 1 h. The sections were incubated overnight at 4°C with one of the following primary antibodies (Rockland Immunochemicals Inc., Gilbertsville, PA, USA): rabbit anti-human collagen I (1:200, cat. no. 600-401-103-0.5), rabbit anti-human collagen III (1:200, cat. no. 600-401-105-0.1), rabbit anti-human collagen IV (1:200, cat. no. 600-401-106-0.1), or rabbit anti-human fibronectin (1:200, cat. no. 600-117-0.1). All antibodies were diluted with blocking solution (1:10). After five rinses in phosphate-buffered saline, donkey anti-rabbit IgG-conjugated with Cy3 (cat. no. 711-165-152, Jackson Immunoresearch, West Grove, PA, USA) was added for 1 h in the dark at room temperature. Following washes with phosphate-buffered saline, the sections were mounted in 90% glycerol/10% Tris 1 M, and images were captured through a confocal microscope (Zeiss LSM 510, Carl Zeiss Inc., Göttingen Germany), × 40 objective, and × 400 original magnification. All confocal settings were determined at the beginning of the imaging session and remained unchanged. For quantitative analysis, the images were captured at 8 bits and analyzed in a gray scale. Four images were captured from each kidney region and three measurements were obtained for each image. Scion Image Beta 4.02 software (Scion Corporation, NIH-USA) was used to quantify fluorescence intensity and area. Background fluorescence was subtracted from the region of interest. The intensity of fluorescence corresponded to the unit 'gray level,' varying from 0 (black) to 255 (white), as an average of the area (sum of gray value of all pixels divided by the number of pixels/area).

Immunoblotting. Equal amounts of protein (50 μg) of each kidney sample were prepared for electrophoresis with a sample buffer NuPAGE LDS (Invitrogen Corporation, Carlsbad, CA, USA) plus 10% β-mercaptoethanol, and incubated at 70°C for 10 min. As described earlier,[63] the samples were loaded into bis-Tris NuPAGE 4–12% gels (Invitrogen) and submitted to electrophoresis, followed by transfer to nitrocellulose membranes (Hybond ECL, Amersham Pharmacia Biotech, Chalfont St Giles, UK). Protein loading and efficiency of blot transfer were monitored by staining with Ponceau S (Sigma Chemical, St Louis, MO, USA). The membranes were blocked for 45 min with tris-buffered saline 0.1%Tween-20 plus 5%non-fat milk. The membrane blots were incubated overnight at 4°C with the same antibodies used on immunohistochemistry (anti-collagen I, 1:5000; anti-collagen III, 1:5000; anti-collagen IV, 1:1000; anti-fibronectin, 1:5000; and anti-β-actin, 1:7000), diluted in tris-buffered saline 0.1% Tween-20. The membranes were then washed and incubated for 1 h at room temperature with horseradish peroxidase-conjugated secondary antibody, goat anti-rabbit IgG (1:15,000). The membranes were submitted to chemiluminescent detection with ECL Plus (Amersham Biosciences,

Chalfont St Giles, UK) and visualized on ImageQuant. Densitometric analysis was carried out using Scion Image Beta 4.0.2 software.

Mas distribution in the kidney

Immunofluorescence analysis was carried out in four kidneys from $Mas^{+/+}$ mice to assess the localization of Mas. The same procedures described earlier for immunofluorescence analysis of extracellular matrix proteins were carried out to prepare the kidney sections. Immunofluorescence labeling and quantitative confocal microscopy were then carried out to determine the distribution of Mas in renal tissue, using a specific Mas antibody (Novus Biologicals, Littleton, CO, USA).

RNA expression for AT$_1$ receptor and TGF-β

Total RNA expression of AT$_1$ receptor and TGF-β in the kidney was evaluated by retrotranscription and real-time PCR assays in five animals of each group. Total RNA was prepared using the TRIzol reagent (Invitrogen). RNA samples were reverse transcribed with MML-V (Invitrogen). The endogenous hypoxanthine guanine phosphoribosyltransferase (HPRT, internal control), AT$_1$, and TGF-β cDNA were amplified using specific primers and the SYBR Green reagent (Applied Biosystem, Carlsbad, CA, USA) in an ABI Prism 7000 platform (Applied Biosystem). AT$_1$ primers: forward, ATGGCTGGCATTTTGTCTGG; reverse, GTTGAGTTGGTCTCAGA CAC. TGF-β primers: forward, GGTTCATGTCATGGATGGTGC; reverse, TGACGTCACTGGAGTTGTAGGG. HPRT primers: forward, GTTGGATACAGGCCAGACTTTGTT; reverse, GATTCAAC TTGCGCTCATCTTAGGC.

Statistical analysis

Data were expressed as mean ± s.e.m. or median. Values with Gaussian distribution were analyzed using the unpaired Student's *t*-test. Non-Gaussian variables were expressed as medians and compared using the Mann–Whitney test. Values of $P < 0.05$ were considered significant and adjusted by Bonferroni's correction according to the number of comparisons.

REFERENCES

1. Zaman MA, Oparil S, Calhoun DA. Drugs targeting the renin angiotensin aldosterone system. *Nat Rev Drug Discov* 2002; **1**: 621–636.
2. Ferrario CM, Chappell MC. Novel angiotensin peptides. *Cell Mol Life Sci* 2004; **61**: 2720–2727.
3. Simões e Silva AC, Pinheiro SVB, Pereira RM *et al*. The therapeutic potential of Angiotensin-(1–7) as a novel renin angiotensin system mediator. *Mini-Rev Med Chem* 2006; **6**: 603–609.
4. Santos RAS, Ferreira AJ, Simões e Silva AC. Recent advances in the angiotensin-converting enzyme 2-angiotensin(1–7)-Mas axis. *Exp Physiol* 2008; **93**: 519–527.
5. Albiston AL, McDowall SG, Matsacos D *et al*. Evidence that the angiotensin IV (AT(4)) receptor is the enzyme insulin-regulated aminopeptidase. *J Biol Chem* 2001; **276**: 48623–48626.
6. Donoghue M, Hsieh F, Baronas E *et al*. A novel angiotensin-converting enzyme-related carboxypeptidase (ACE2) converts angiotensin I to angiotensin-(1–9). *Circ Res* 2000; **87**: 1–9.
7. Tipnis SR, Hooper NM, Hyde R *et al*. A human homolog of Angiotensin-converting enzyme. Cloning and functional expression as a captopril-insensitive carboxypeptidase. *J Biol Chem* 2000; **275**: 33238–33243.
8. Santos RAS, Simões e Silva AC, Maric C *et al*. Angiotensin-(1–7) is an endogenous ligand for the G-protein coupled receptor Mas. *Proc Natl Acad Sci USA* 2003; **100**: 8258–8263.
9. Simões e Silva AC, Diniz JS, Regueira-Filho A *et al*. The Renin Angiotensin System in childhood hypertension: Selective increase of Angiotensin-(1–7) in essential hypertension. *J Pediatr* 2004; **145**: 93–98.
10. Simões e Silva AC, Diniz JS, Pereira RM *et al*. Circulating Renin Angiotensin System in childhood chronic renal failure: Marked increase of Angiotensin-(1–7) in end-stage renal disease. *Pediatr Res* 2006; **60**: 734–739.
11. Maia LG, Ramos MC, Fernandes L *et al*. Angiotensin-(1–7) antagonist A-779 attenuates the potentiation of bradykinin by captopril in rats. *J Cardiovasc Pharmacol* 2004; **43**: 685–691.
12. Höcht C, Gironacci MM, Mayer MA *et al*. Involvement of angiotensin-(1–7) in the hypothalamic hypotensive effect of captopril in sinoaortic denervated rats. *Regul Pept* 2008; **146**: 58–66.
13. Ishiyama Y, Gallagher PE, Averill DB *et al*. Upregulation of angiotensin-converting enzyme 2 after myocardial infarction by blockade of angiotensin II receptors. *Hypertension* 2004; **43**: 970–976.
14. Kostenis E, Milligan G, Christopoulos A *et al*. G-protein-coupled receptor Mas is a physiological antagonist of the angiotensin II type 1 receptor. *Circulation* 2005; **111**: 1806–1813.
15. Canals M, Jenkins L, Kellett E *et al*. Up-regulation of the angiotensin II type 1 receptor by the Mas proto-oncogene is due to constitutive activation of Gq/G11 by Mas. *J Biol Chem* 2006; **281**: 16757–16767.
16. Santos RAS, Castro CH, Gava E *et al*. Impairment of *in vitro* and *in vivo* heart function in angiotensin-(1–7) receptor Mas knockout mice. *Hypertension* 2006; **47**: 996–1002.
17. Xu P, Costa-Goncalves AC, Todiras M *et al*. Endothelial dysfunction and elevated blood pressure in Mas gene-deleted mice. *Hypertension* 2008; **51**: 574–580.
18. Costa Gonçalves AC, Leite R, Fraga-Silva RA *et al*. Evidence that the vasodilator angiotensin-(1–7)-Mas axis plays an important role in erectile function. *Am J Physiol Heart Circ Physiol* 2007; **293**: H2588–H2596.
19. Fraga-Silva RA, Pinheiro SV, Gonçalves AC *et al*. The antithrombotic effect of angiotensin-(1–7) involves Mas-mediated NO release from platelets. *Mol Med* 2008; **14**: 28–35.
20. Santos SH, Fernandes LR, Mario EG *et al*. Mas deficiency in FVB/N mice produces marked changes in lipid and glycemic metabolism. *Diabetes* 2008; **57**: 340–347.
21. Hansen PB, Yang T, Huang Y *et al*. Plasma renin in mice with one or two renin genes. *Acta Physiol Scand* 2004; **181**: 431–437.
22. Navar LG, Nishiyama A. Why are angiotensin concentrations so high in the kidney? *Curr Opin Nephrol Hypertens* 2004; **13**: 107–115.
23. Brewster UC, Perazella MA. The renin-angiotensin-aldosterone system and the kidney: effects on kidney disease. *Am J Med* 2004; **116**: 263–272.
24. Arendshorst WJ, Brannstrom K, Ruan X. Actions of angiotensin II on the renal microvasculature. *J Am Soc Nephrol* 1999; (Suppl 11): S149–S161.
25. Hall JE, Brands MW, Henegar JR. Angiotensin II and long-term arterial pressure regulation: the overriding dominance of the kidney. *J Am Soc Nephrol* 1999; (Suppl 12): S258–S265.
26. Ren Y, Garvin JL, Carretero AO. Vasodilator action of angiotensin-(1–7) on isolated rabbit afferent arterioles. *Hypertension* 2002; **39**: 799–802.
27. Sampaio WO, Nascimento AA, Santos RAS. Systemic and regional hemodynamics effects of angiotensin-(1–7) in rats. *Am J Physiol* 2003; **284**: H1985–H1994.
28. Gironacci MM, Adler-Graschinsky E, Pena C *et al*. Effects of angiotensin II and angiotensin-(1–7) on the release of [³H]norepinephrine from rat atria. *Hypertension* 1994; **24**: 457–460.
29. Frokiaer J, Nielsen S, Knepper MA. Molecular physiology of renal aquaporins and sodium transporters: Exciting approaches to understand regulation of renal water handling. *J Am Soc Nephrol* 2005; **16**: 2827–2829.
30. Oudit GY, Herzenberg AM, Kassiri Z *et al*. Loss of angiotensin-converting enzyme-2 leads to the late development of angiotensin II-dependent glomerulosclerosis. *Am J Pathol* 2006; **168**: 1808–1820.
31. Pereira RM, Santos RAS, Teixeira MM *et al*. The Renin Angiotensin System in a rat model of hepatic fibrosis: Evidence for a protective role of Angiotensin-(1–7). *J Hepatol* 2007; **46**: 674–681.
32. Kuncio GS, Neilson EG, Haverty TP. Mechanisms of tubulointerstitial fibrosis. *Kidney Int* 1992; **39**: 550–556.
33. Harris RC, Neilson EG. Toward a unified theory of renal progression. *Annu Rev Med* 2006; **57**: 365–380.

34. Fakhouri F, Placier S, Ardaillou R *et al.* Angiotensin II activates collagen type I gene in the renal cortex and aorta of transgenic mice through interaction with endothelin and TGF-β. *J Am Soc Nephrol* 2001; **12**: 2701–2710.

35. Remuzzi A, Gagliardini E, Donadoni C *et al.* Effect of angiotensin II antagonism on the regression of kidney disease in the rat. *Kidney Int* 2002; **62**: 885–894.

36. Boffa JJ, Lu Y, Placier S *et al.* Regression of renal vascular and glomerular fibrosis: Role of Angiotensin II receptor antagonism and matrix metalloproteinases. *J Am Soc Nephrol* 2003; **14**: 1132–1144.

37. Chen S, Lee JS, Iglesias-de la Cruz MCI *et al.* Angiotensin II stimulates α3(IV) collagen production in mouse podocytes via TGF-β and VEGF signaling: implications for diabetic glomerulopathy. *Nephrol Dial Transplant* 2005; **20**: 1320–1328.

38. Ma LJ, Fogo A. Modulation of glomerulosclerosis. *Semin Immunopathol* 2007; **29**: 385–395.

39. Border WA, Okuda S, Languino LR *et al.* Suppression of experimental glomerulonephritis by antiserum against transforming growth factor beta 1. *Nature* 1990; **346**: 371–374.

40. Wolf G. Renal injury due to renin-angiotensin-aldosterone system activation of the transforming growth factor-beta pathway. *Kidney Int* 2006; **70**: 1914–1919.

41. August P, Suthanthiran M. Transforming growth factor beta and progression of renal disease. *Kidney Int* 2003; (Suppl 87): S99–S104.

42. Liu Y. Renal fibrosis: new insights into the pathogenesis and therapeutics. *Kidney Int* 2006; **69**: 213–217.

43. Tallant EA, Ferrario CM, Gallagher PE. Angiotensin-(1–7) inhibits growth of cardiac myocytes through activation of the Mas receptor. *Am J Physiol* 2005; **289**: 1560–1566.

44. Machado RD, Ferreira MA, Belo AV *et al.* Vasodilator effect of angiotensin-(1–7) in mature and sponge-induced neovasculature. *Regul Pept* 2002; **107**: 105–113.

45. Tallant EA, Clark MA. Molecular mechanisms of inhibition of vascular growth by angiotensin-(1–7). *Hypertension* 2003; **42**: 574–579.

46. Gallagher PE, Tallant EA. Inhibition of human lung cancer cell growth by angiotensin-(1–7). *Carcinogenesis* 2004; **25**: 2045–2052.

47. Iwata M, Cowling RT, Gurantz D *et al.* Angiotensin-(1–7) binds to specific receptors on cardiac fibroblasts to initiate antifibrotic and antitrophic effcts. *Am J Physiol* 2005; **289**: 2356–2363.

48. Su Z, Zimpelmann J, Burns KD. Angiotensin-(1–7) inhibits angiotensin II-stimulated phosphorylation of MAP kinases in proximal tubular cells. *Kidney Int* 2006; **69**: 2212–2218.

49. Wysocki J, Ye M, Soler MJ *et al.* ACE and ACE2 activity in diabetic mice. *Diabetes* 2006; **55**: 2132–2139.

50. Ye M, Wysocki J, William J *et al.* Glomerular localization and expression of Angiotensin-converting enzyme 2 and Angiotensin-converting enzyme: implications for albuminuria in diabetes. *J Am Soc Nephrol* 2006; **17**: 3067–3075.

51. Wong DW, Oudit GY, Reich H *et al.* Loss of angiotensin-converting enzyme-2 (Ace2) accelerates diabetic kidney injury. *Am J Pathol* 2007; **171**: 438–451.

52. Soler MJ, Wysocki J, Ye M *et al.* ACE2 inhibition worsens glomerular injury in association with increased ACE expression in streptozotocin-induced diabetic mice. *Kidney Int* 2007; **72**: 614–623.

53. Anderson S, Meyer TW, Rennke HG *et al.* Control of glomerular hypertension limits glomerular injury in rats with reduced renal mass. *J Clin Invest* 1985; **76**: 612–619.

54. Taal MW, Brenner BM. Renoprotective benefits of RAS inhibition: from ACEI to angiotensin II antagonists. *Kidney Int* 2000; **57**: 1803–1817.

55. Azizi M, Ménard J. Combined blockade of the Renin Angiotensin System with Angiotensin-converting enzyme inhibitors and Angiotensin II type 1 receptor antagonists. *Circulation* 2004; **109**: 2492–2499.

56. Codreanu I, Perico N, Remuzzi G. Dual blockade of the renin-angiotensin system: the ultimate treatment for renal protection? *J Am Soc Nephrol* 2005; (Suppl 1): S34–S38.

57. Qi Z, Whitt I, Mehta A *et al.* Serial determination of glomerular filtration rate in conscious mice using FITC-Inulin clearance. *Am J Physiol Renal Physiol* 2004; **286**: 590–596.

58. Davidson WD, Sackner MA. Simplification of the anthrone method for the determination of inulin in clearance studies. *J Lab Clin Med* 1963; **62**: 351–356.

59. Gervais M, Demolis SP, Domerg V *et al.* Systemic and regional hemodynamics assessment in rats with fluorescent microspheres. *J Cardiovasc Pharmacol* 1999; **33**: 425–432.

60. Glenny RW, Bernard S, Brinkley M. Validation of fluorescent-labeled microspheres for measurement of regional organ perfusion. *J Appl Physiol* 1993; **74**: 2585–2597.

61. Van Oosterhout MFM, Willigers MM, Renaman RS *et al.* Fluorescent microspheres to measure organ perfusion: validation of a simplified sample processing technique. *Am J Physiol Heart Circ Physiol* 1995; **269**: H725–H733.

62. de Oliveira GV, Sanford AP, Murphy KD *et al.* Growth hormone effects on hypertrophic scar formation: a randomized controlled trial of 62 burned children. *Wound Repair Regen* 2004; **12**: 404–411.

63. Souza BR, Motta BS, Rosa DVF *et al.* DARPP-32 and NCS-1 expression is not altered in brains of rats treated with typical or atypical antipsychotics. *Neurochem Res* 2008; **33**: 533–538.